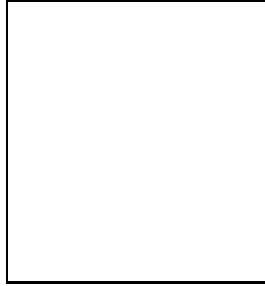


# WEAK WEAK LENSING: HOW ACCURATELY CAN SMALL SHEARS BE MEASURED?

K. KUIJKEN

*Kapteyn Instituut, PO Box 800, 9700 AV Groningen, The Netherlands*



Now that weak lensing signals on the order of a percent are actively being searched for (cosmic shear, galaxy-galaxy lensing, large radii in clusters...) it is important to investigate how accurately weak shears can be determined. Many systematic effects are present, and need to be understood. I show that the Kaiser et al. technique can leave residual systematic errors at the percent level (through imperfect PSF anisotropy correction), and present an alternative technique which is able to recover shears a factor of ten weaker.

## 1 Introduction

Weak lensing has evolved in the last ten years into a quantitative tool in cosmology. The goal is no longer to demonstrate a convincing detection of the effect, but to make real measurements of the shear, and turn these into real measurements of the projected mass density in a given direction.

An important aspect of this quantitative work is to control systematic effects. While it is now relatively straightforward to demonstrate convincingly a coherent alignment of galaxy distortions around a massive foreground cluster, for example, it is much harder to quantify the amount of this shear in the presence of seeing, camera distortions, or uncertain redshift distributions of the source galaxies. As an example, Fig 1 shows the weak shear field around the  $z \sim 0.83$  cluster MS1054-03 from a 6-exposure WFPC2 mosaic<sup>5</sup>. In order to come to this shear field, many of the effects to be discussed in the following section had to be quantified and corrected for.

Nevertheless, this is an example of a rather strong lensing effect, shears around 10%. The field is also evolving in the direction of working with weaker and weaker gravitational shears. Ground-based cameras now have wider fields which allow the outskirts of clusters to be observed efficiently. For a singular isothermal sphere model the shear falls with radius as  $r^{-1}$ , and it is

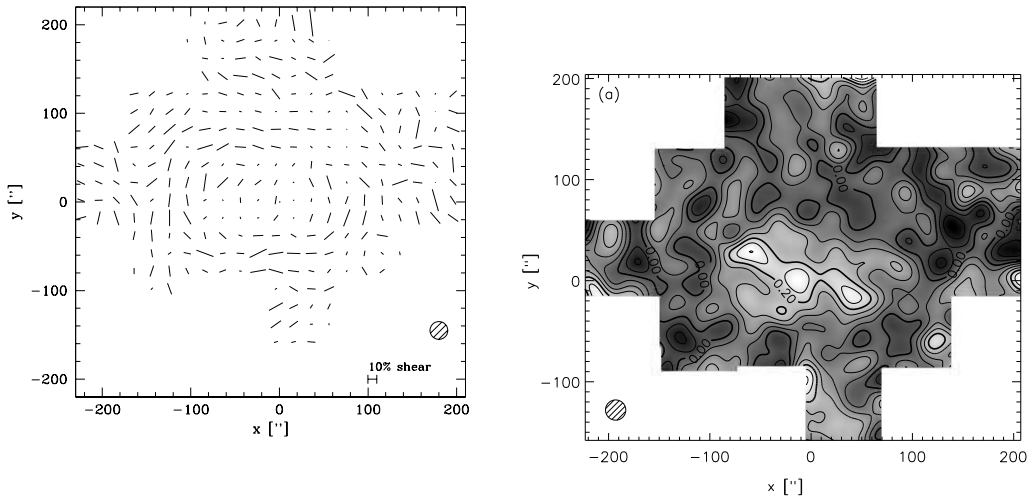


Figure 1: Weak Lensing shear field (top), and mass map (right) of the  $z = 0.83$  cluster MS1054-03 by Hoekstra et al (2000).

now routinely possible to reach the region of clusters where the shear should be around 1%. While formally signal-to-noise is a very weak function of radius (the shear drops outwards, but the number of available background galaxies whose shapes may be averaged to yield a shear estimate increases with radius), systematic effects become a serious concern. Also lower-mass clusters and groups, much more representative of the universe than the massive X-ray clusters, are now within reach (Hoekstra et al 2000).

In clusters there is at least the independent sanity check of making sure that the shear is aligned roughly with the observed cluster. Lately, though, a lot of effort has gone into the search for cosmic shear, which is the lensing effect caused by large-scale structure<sup>14,1,15,9</sup>). Here the measurement is rather similar to the early cosmic background radiation anisotropy experiments, and constitutes the search for an excess variance. The effect is also on the level of a percent shear or less, but its geometry is a priori unclear.

Also galaxy-galaxy lensing is now being carried out with enormous numbers of lens-source pairs, and formal averaging statistics allow shears of well below a percent to be measured (see Fisher, this conference). As in galaxy-galaxy lensing the lens and source are rather close together on the sky, any large-scale systematic distortion cancels out to first order, making it a little less susceptible to residual systematics.

## 2 Systematic errors

The image of a distant galaxy that we record on a CCD is a

- charge-transferred,
- pixellated,
- camera-distorted,
- atmospherically blurred,
- gravitationally lensed,
- random-shape,
- randomly-oriented

galaxy. We can only extract the lensing information if we can control all these other effects, either by avoiding them, or by measuring and correcting for their effects.

Fortunately the sky contains a number of calibrators, stars in the field. These are for our purposes point-like, and so measure the smearing effects of atmosphere and optics simultaneously with the galaxies. Galaxy orientations on the sky are random as far as we know. CCD effects can be calibrated by observing at different orientations with respect to the pixel grid, or by using totally different cameras altogether. The distortion of the camera can be calibrated with astrometric standard fields, or by comparing offset exposures.

In principle, therefore, it looks as if the required information exists to disentangle the effects of gravitational lensing from the other ones. Assuming for the moment that this has been done, this means that for each background galaxy an estimate for the distortion can be obtained.

The distortions  $g_i$ , ( $i = 1, 2$ ) are equivalent to the axis ratio and major axis orientation observed when an intrinsically round source is lensed.  $g$  is related to the distortion matrix

$$\begin{pmatrix} 1 - \kappa - \gamma_1 & -\gamma_2 \\ -\gamma_2 & 1 - \kappa + \gamma_1 \end{pmatrix} \quad (1)$$

through  $g_i = \gamma_i/(1 - \kappa)$ . Here  $\gamma$  is the gravitational shear, and  $\kappa$  the convergence. The latter is a measure of the surface mass density in the lens plane, and is the goal of weak lensing.

There are several complications in converting the observed distortions into a projected mass density.

- *PSF*. The Point Spread Function affects galaxy images in various ways. If the PSF is anisotropic, it will imprint this anisotropy onto the observed image. On the other hand, since it has a finite width it will tend to increase the size of faint images. As the PSF acts as a convolution, galaxies of different size are affected by PSF in different degrees.
- *Camera Shear*. The camera maps the sky onto the focal plane, but often does not do this without introducing some distortion. It is easy to show that such a distortion produces shear, and that this acts as a simple additive effect onto the observed gravitational shear.
- $(1-\kappa)$ . The measured distortion is a combination of  $\gamma$  and  $\kappa$ . To derive the shear it is therefore necessary to have an estimate of the convergence. This is a fundamental limitation of weak lensing, and is known as the mass-sheet degeneracy<sup>12</sup>. Usually one assumes that the mass distribution at the outer edges of the field follows some simple model (zero, singular isothermal, ...), or one leaves the uncertain  $\kappa$  zeropoint in the result<sup>6</sup>.
- *Redshift Distribution*. The deflection angle in lensing depends on the relative distances between observer, source and lens. As the source distances are usually unknown, or only known statistically, the lensing angles, and hence the shears, need to be corrected to infinite source redshift. This correction factor is usually referred to as the  $\beta$  factor:

$$\gamma(\text{observed}) = \beta\gamma(\text{infinite source distance}), \quad (2)$$

where  $\beta$  is the ratio of lens to source distance. The effect is most important for distant cluster work, or for situations where lenses and sources are distributed similarly down the line of sight as in cosmic shear measurements. Source galaxies used for lensing are usually so faint that they are beyond the reach of spectroscopic redshift surveys, so models or photometric redshift studies need to be used. The analysis performed for MS1054 (fig. 1) relied on the HDF redshift distributions<sup>3,2</sup>. A discrepancy of around 10%, which may well be a form of cosmic variance, exists between the two Deep Fields.

- $\beta$  spread. Even once the mean redshift of the sources is determined, a second-order effect exists which depends on the width of the distribution of  $\beta$ . This is because the distortion

is not linear in  $\kappa$ , and so the observed distortion is

$$g(\text{observed}) = \frac{\gamma(\text{observed})}{1 - \kappa(\text{observed})} = \frac{\beta\gamma}{1 - \beta\kappa} = \beta\gamma + \beta^2\kappa\gamma + O(\kappa^2) \quad (3)$$

which, when averaged over source galaxies with different redshift requires knowledge of  $\overline{\beta^2}$ , and hence of the variance of the  $\beta$ -distribution<sup>5,13</sup>.

Most of these effects are important when it comes to properly calibrating the strength of a detected distortion pattern, and turning it into a real mass.

The correction for PSF effects is technically the most difficult of these steps. The most extensively used method is the KSB<sup>8</sup> method, which can be considered the current ‘industry standard.’ Of the many weak lensing results that have been obtained to date<sup>11</sup>, most have employed this technique.

### 3 Tests of the KSB method

The KSB method uses a combination of centered second image moments as its shape statistic. This is a logical choice: these moments measure the orientation and elongation of an ellipse, which is a reasonable first approximation to galaxy images. KSB worked out how these image moments, and the shape statistics derived from them, behave under various distorting effects. The result is a formalism for deriving ‘polarizabilities’, matrices which express the response of the image polarization

$$(e_1, e_2) \equiv \left( \frac{I_{xx} - I_{yy}}{I_{xx} + I_{yy}}, \frac{2I_{xy}}{I_{xx} + I_{yy}} \right) \quad (4)$$

to gravitational shear, and to PSF smearing. KSB show how these polarizabilities can themselves be written as combinations of higher-order image moments. The image moments  $I_{ij}$  of the galaxy image intensity  $f(x, y)$  are computed with a circular weight function  $W(r)$ , to prevent poisson noise from dominating the measurements:

$$I_{ij} = \int dx dy f(x, y) W(r). \quad (5)$$

In particular, the effect on  $(e_1, e_2)$  of a distant galaxy under smearing by an anisotropic PSF is given by

$$\delta e_\alpha = P_{\alpha\beta}^{\text{sm}} p_\beta \quad (6)$$

where  $p$  is the PSF anisotropy,  $(I_{xx} - I_{yy}, 2I_{xy})$ , this time constructed from unweighted second moments.

This formalism works very well, but not perfectly. An example is shown in figure 2, which is the average of two normalized gaussians, of  $(x, y)$ -variance  $(1.1, 1)$  and  $(3.9, 4)$  respectively. The total variances in  $x$  and  $y$  of this PSF are the same, i.e. its anisotropy  $p$  is zero. No matter what the polarizability of a source, therefore, the KSB formulae would predict no effect on the polarization of a source after convolution with this PSF. However, as figure 2 shows, this is not correct, because of the radial weight function used in the computation of the polarizations. Errors of the order of a percent in the image polarization can result.

A set of simulations illustrating such systematic effects is shown in fig. 3. A more extensive discussion is given in Kuijken (1999)<sup>10</sup>.

The residual systematics are not fundamental: the PSF is known perfectly, so all required information is there. It is instead a consequence of a mathematical assumption made by KSB (that the PSF can be written as a convolution of a very compact anisotropic kernel with a more extended, round function) to enable the polarizabilities to be constructed.

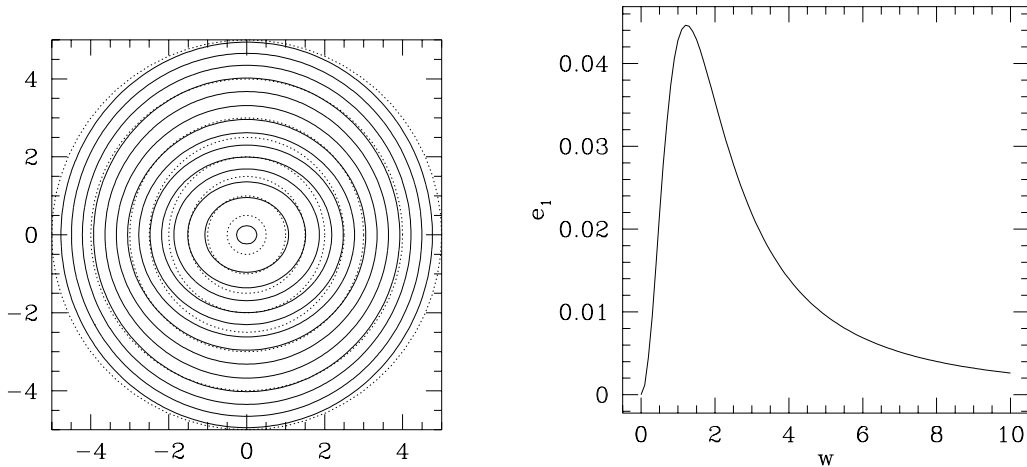


Figure 2: Left: An example of a PSF which is isotropic in its second moments, but not intrinsically. Right: the polarization of this PSF when it is measured with different gaussian weight functions ( $1\text{-}\sigma$  radius  $w$ ).

#### 4 An alternative algorithm: Constant Ellipticity Objects

Alternative algorithms have been developed, but none are in as wide a use as KSB. One class is based on reconvolving the data with a circularizing kernel<sup>5,7</sup>. This is a rather direct way to reduce PSF effects, but creates correlated noise and, unavoidably, somewhat degrades the data.

An alternative algorithm<sup>10</sup> does not rely on modelling the second moments, but instead is a direct fit of the sources to a sheared, intrinsically circular source, convolved with the PSF. As a sheared circular source has ellipticity which is constant with radius, the algorithm has been dubbed Constant Ellipticity Objects (CEO).

An exhaustive discussion will not be given here, as the details may be found in the original paper. The essence of the results are as follows:

- When the sources are intrinsically round, the algorithm recovers the shears from noise-free images, even for very anisotropic PSF's which the KSB technique does not correct to better than a percent.
- When Poisson noise is added to simulated images, the best-fit shears are unbiased, and the scatter is very similar to the KSB method. (This shows that the KSB method, even though it only uses a few moments of each image, is close to optimal in the amount of information it uses from the images).
- When the algorithm is applied to sources which are not intrinsically round, but which are made to look like disk/bulge systems seen at various orientations and inclinations, the ensemble average of the individual shear estimates is within a few tenths of a percent of the correct value. I.e., even though the individual galaxies are fit with a model which is not correct (they are not intrinsically round) the errors made average out (see Fig 4).

#### 5 Consistency Checks

However shears are measured, it is important to be able to perform consistency checks on the results. Below are listed a set of tests that can be performed.

Round galaxy, PSF  $\epsilon$  constant

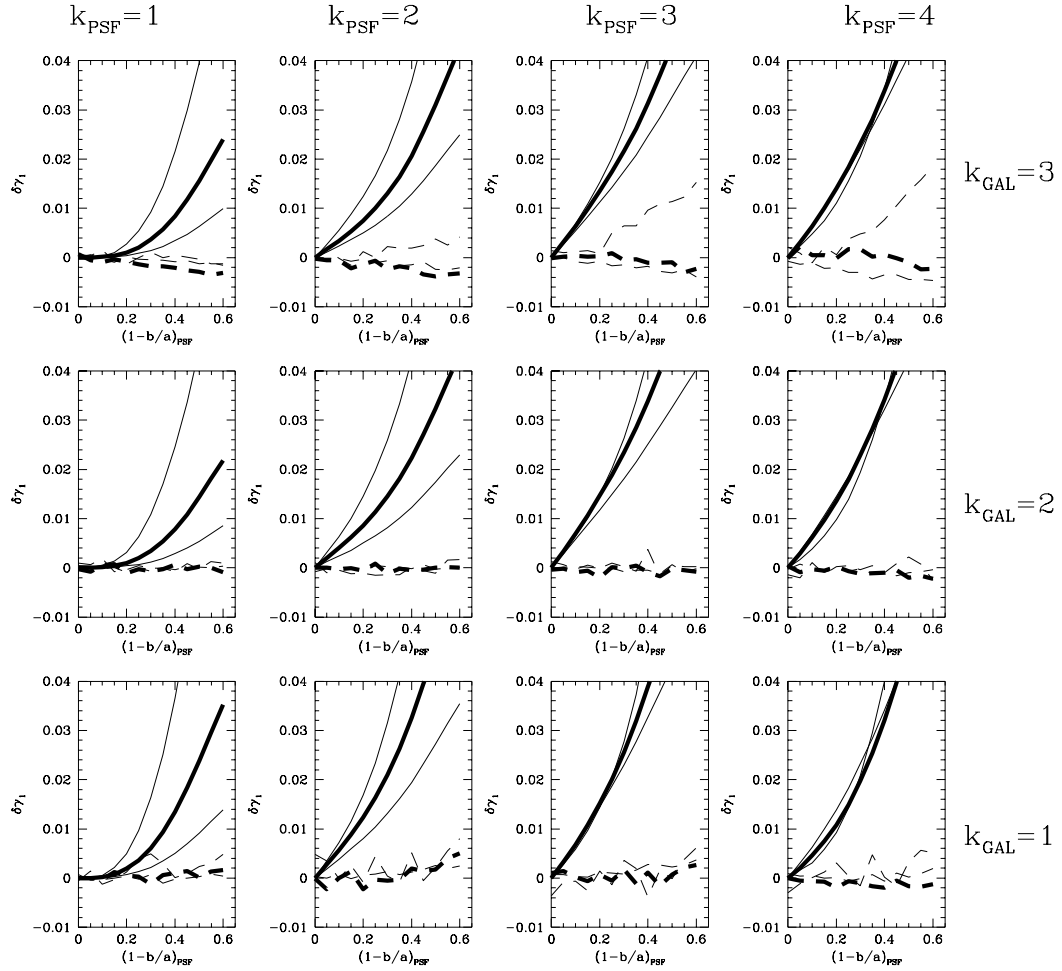


Figure 3: Simulations of the extent to which the KSB (solid lines) and CEO (ashed lines) algorithms corrects an input PSF anisotropy. Double-gaussian PSF's of axis ratio  $b/a$  were convolved with round double-gaussian 'galaxies', and analysed with both algorithms.  $k$  is the ratio of the dispersions of the two gaussian components:  $k = 2$  is roughly exponential,  $k = 3$  is roughly de vaucouleurs. No lensing was simulated here, so the derived shears should be zero. Several percent residuals remain for the most non-gaussian PSF's.

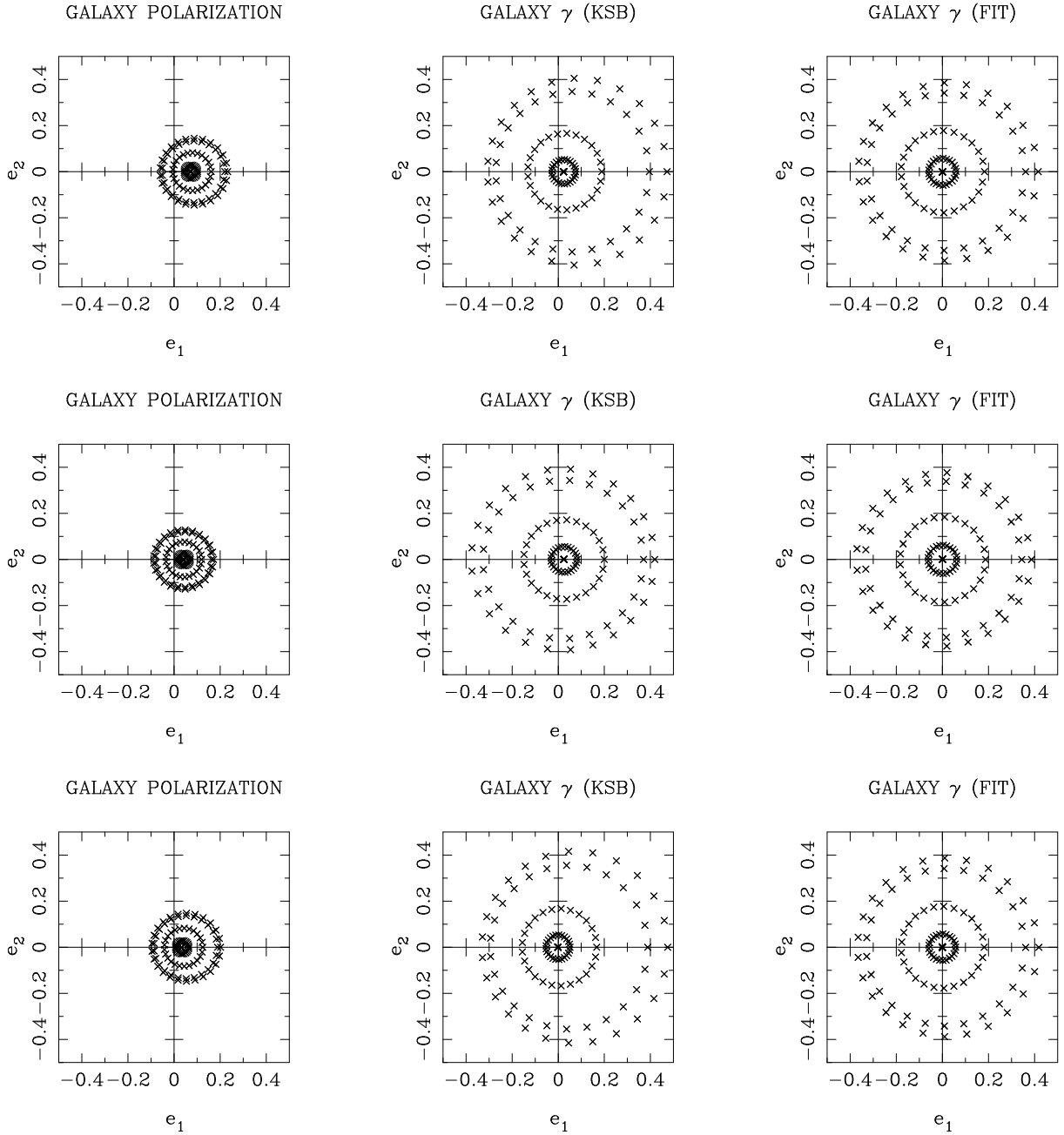


Figure 4: Various galaxy models, of different elongations and orientations, convolved with anisotropic PSFs and then analysed with the CEO and KSB algorithms. Left column: raw polarizations. Middle column: shear deduced from the KSB formalism. Right column: shear deduced from the CEO method. The different rows correspond to different radial ellipticity profiles of the PSF.

- Transform corrected galaxy polarizations  $e_1 \rightarrow e_2$ ;  $e_2 \rightarrow -e_1$ . Surface mass density should now be consistent with zero.
- There should be no correlations between  $\gamma$  and  $e^*$ , the polarization of the stars used in the correction for PSF effects.
- Results should be independent of wavelength observed in, or instrument.
- Shear fields should not rotate with the instrument or detectors.
- Smear image data with a typical PSF, and re-analyse these images. Results may be a little noisier, but should be consistent with original result. [this tests algorithm, not data]
- Vary the weight function radius in KSB
- Track the signal as a function of source size. Smaller sources are more sensitive to PSF

## 6 Summary

Weak lensing work is moving into the regime of very weak signals. Lensing by large-scale structure, the outskirts of clusters, and low-mass galaxy groups and individual galaxies are all being targeted. Particularly the first results being reported elsewhere at this conference on the detection of lensing by large-scale structure are very exciting.

Measuring these very weak distortions is a tricky business, because many other effects need to be characterized and corrected for. I have described a new algorithm, which performs very well on test data, which is able to reduce systematic uncertainties associated with the correction for PSF anisotropy considerably. Applications on real data are in progress.

## Acknowledgments

This work, and this conference visit, was supported by the TMR Network ‘‘Gravitational Lensing: New Constraints on Cosmology and the Distribution of Dark Matter’’ of the EC under contract No. ERBFMRX-CT97-0172.

## References

- [1] Bacon, D., Refregier, A., and Ellis, R. 2000, MNRAS, in press (astro-ph/0003008)
- [2] Chen, H.-W., et al. 1998, preprint (astro-ph/9812339)
- [3] Fernandez-Soto, A., Lanzetta, K. M. and Yahil, A. 1999, ApJ, 513, 34
- [4] Hoekstra, H., Franx, M., Kuijken, K. and Squires, G. 1998, ApJ, 504, 636
- [5] Hoekstra, H., Franx, M. and Kuijken, K. 2000, ApJ, 532, 88
- [6] Kaiser, N. 1995, ApJL, 439, L1
- [7] Kaiser, N. 2000, ApJ, 537, 555
- [8] Kaiser, N., Squires, G. and Broadhurst, T. 1995, ApJ, 449, 460
- [9] Kaiser, N., Wilson, G. and Luppino, G.A., ApJL, submitted (astro-ph/0003338)
- [10] Kuijken, K. 1999, A&A, 352, 355
- [11] Mellier, Y. 1999, ARAA, 37, 127
- [12] Schneider, P., Ehlers, J. ;. and Falco, E. E. 1992, Gravitational Lenses. Springer-Verlag:Berlin
- [13] Seitz, C. and Schneider, P. 1997, A&A, 318, 687
- [14] Van Waerbeke, L. and 12 colleagues 2000, A&A, 358, 30
- [15] Wittman, D.M., Tyson, J.A., Kirkman, D., Dell’Antonio, I. and Bernstein, G. 2000, Nature, in press (astro-ph/0003014)